

## Influence of microstructure on local conductivities in $\text{La}_{0.7}\text{Ce}_{0.3}\text{MnO}_3$ thin film

This content has been downloaded from IOPscience. Please scroll down to see the full text.

2009 J. Phys.: Conf. Ser. 150 042164

(<http://iopscience.iop.org/1742-6596/150/4/042164>)

View [the table of contents for this issue](#), or go to the [journal homepage](#) for more

Download details:

IP Address: 27.34.254.60

This content was downloaded on 22/02/2017 at 05:04

Please note that [terms and conditions apply](#).

You may also be interested in:

[Electroresistive effects in electron doped manganite  \$\text{La}\_{0.7}\text{Ce}\_{0.3}\text{MnO}\_3\$  thin films](#)

Kavita Bajaj, John Jesudasan, Vivas Bagwe et al.

[Correlation between effects of electric current and magnetic field on transport properties of electron-doped manganite  \$\text{La}\_{0.7}\text{Ce}\_{0.3}\text{MnO}\_3\$  thin films](#)

Kavita Bajaj, John Jesudasan, Vivas Bagwe et al.

[Migration of Metals on Graphite in Scanning Tunneling Microscopy](#)

Masanori Ohto, Satoru Yamaguchi and Keiji Tanaka

[Rewritable Near-Field Optical Recording on Photochromic Thin Films](#)

Mitsuo Hamano and Masahiro Irie

[Current-processing-induced anisotropic conduction in manganite films](#)

Y. W. Xie, J. R. Sun, D. J. Wang et al.

[Electron tunnelling through a quantifiable barrier of variable width](#)

A F G Wyatt, H Bromberger, J Klier et al.

[A Study of Electron Loading in the Accelerating Tube of Van de Graaff Generator](#)

Hsu Chu-Chung, Tsutomu Thei, Takemi Nakagawa et al.

# Influence of microstructure on local conductivities in $\text{La}_{0.7}\text{Ce}_{0.3}\text{MnO}_3$ thin film

S Rößler<sup>1</sup>, J Jesudasan<sup>2</sup>, K Bajaj<sup>2</sup>, P Raychaudhuri<sup>2</sup>, F Steglich<sup>1</sup> and S Wirth<sup>1</sup>

<sup>1</sup> Max Planck Institute for Chemical Physics of Solids, Nöthnizer Straße 40, 01187 Dresden, Germany

<sup>2</sup> TIFR, Dept. of Condensed Matter Physics and Materials Science, Mumbai 400005, India

E-mail: roessler@cpfs.mpg.de

**Abstract.** We report on scanning tunneling microscopy and spectroscopy (STM/S) studies of electron doped  $\text{La}_{0.7}\text{Ce}_{0.3}\text{MnO}_3/\text{LaAlO}_3$  thin films grown by pulsed laser deposition. Atomic force microscopy of these films reveals an average grain size of  $\sim 100$  nm. Spatially resolved STS maps in the metallic state, i.e., well below the metal-insulator transition temperature, show phase separation on a length scale of several nanometers. The conductance maps indicate a correlation between the phase separation and the microstructure of the films. The results demonstrate that the local strain as well as the morphology of thin films have a strong influence on the local conductivities which complicates the search for an intrinsic phase separation in manganite thin films.

## 1. Introduction

Colossal magnetoresistive manganites offer rich physics due to competing interactions. They crystallize in a perovskite structure with the general formula of  $\text{Ln}_{1-x}\text{A}_x\text{MnO}_3$ , where  $\text{Ln}$  is a trivalent lanthanide and  $\text{A}$  is usually a divalent alkaline earth ion. Such a partial substitution of  $\text{Ln}$  by  $\text{A}$  yields hole doping and a mixed valence of  $\text{Mn}^{3+}$  and  $\text{Mn}^{4+}$  in these compounds. On the other hand, electron doping can be achieved by substituting  $\text{Ln}$  with a tetravalent  $\text{A}$  ion such as  $\text{Ce}^{4+}$ , which results in a mixed valence of  $\text{Mn}^{3+}$  and  $\text{Mn}^{2+}$ . The electrical and magnetic properties of both hole and electron doped manganites are rather similar [1]. For  $0.2 \lesssim x \lesssim 0.4$ , these compounds undergo a metal-insulator transition as well as a ferromagnetic transition. As a result of the complex interplay of lattice, spin, charge and orbital degrees of freedom, these materials tend to phase separate into metallic (ferromagnetic) and insulating (paramagnetic) states in parts of the phase diagram [2]. Phase separation (PS) in manganites has been observed in several experimental studies, such as electron microscopy [3], photoemission spectroscopy [4] and scanning tunneling microscopy/spectroscopy (STM/S) [5, 6]. The PS was found to persist in the metallic state, also at low temperatures. Our main interest was to investigate whether the PS is an intrinsic property of the materials that is also present in electron doped manganites and whether the PS can be traced down to lowest temperatures  $T$ . Since single phase  $\text{La}_{1-x}\text{Ce}_x\text{MnO}_3$  can only be prepared in thin film form [7], we chose optimally electron doped  $\text{La}_{0.7}\text{Ce}_{0.3}\text{MnO}_3$  (LCeMO) thin films for our studies. Ce-doped manganites are difficult to prepare owing to the relatively small ionic radius of  $\text{Ce}^{4+}$ . Instead of single phase  $\text{La}_{1-x}\text{Ce}_x\text{MnO}_3$ , they tend to form cation deficient  $\text{La}_{1-x}\text{MnO}_3$  and  $\text{CeO}_2$  as a secondary phases

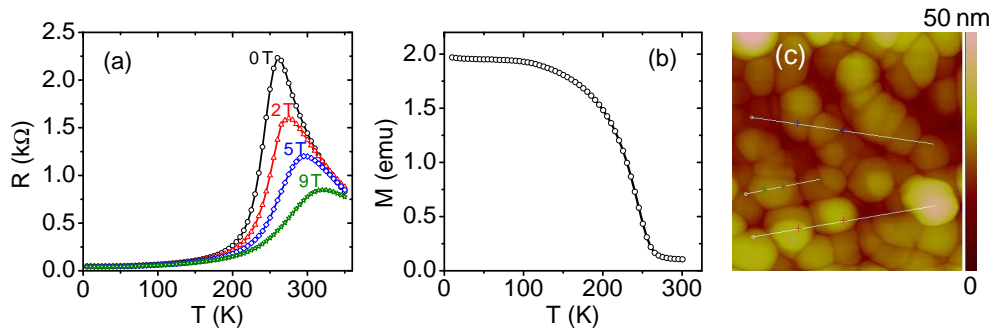


**Figure 1.** (a) Temperature dependence of resistance of a LCeMO thin film measured in different magnetic fields. (b) Magnetization vs temperature in a magnetic field of 0.1 T. (c) AFM image showing the surface morphology of a LCeMO thin film over an area of  $0.5 \times 0.5 \mu\text{m}^2$ .

[8, 9]. However, several groups [7, 10] have successfully grown single phase  $\text{La}_{1-x}\text{Ce}_x\text{MnO}_3$  thin films by pulsed laser deposition. In such films the presence of  $\text{Ce}^{4+}$ ,  $\text{Mn}^{2+}$  and  $\text{Mn}^{3+}$  ions (which suggest electron doping) was confirmed by x-ray absorption [11, 12] and photoemission [12] spectroscopy. Negative high field slope in the field dependence of Hall voltage confirmed that the electrons are the main charge carriers in these films. Contradictory results have been reported by Chang *et al.* [14], who observed electron doping in optical reflectance spectra but hole doping in Hall effect measurements. These results demonstrate that obtaining electron doped LCeMO strongly depends on the film preparation conditions, and a careful tuning of oxygen pressure during the deposition is very crucial. We report here an investigation of the surface conductance in single phase LCeMO thin films using spatially resolved STM/S.

## 2. Experimental

Epitaxial thin films of LCeMO with thickness of about 160 nm were grown on  $\text{LaAlO}_3(100)$  by pulsed laser deposition. The film deposition parameters used here are the same as those in references [7, 11, 13] in which cases electron doping has been confirmed. Electrical and magnetic measurements were carried out in a physical property measurement system (Quantum Design) and a SQUID (superconducting quantum interference device) magnetometer, respectively. Surface morphology was obtained through atomic force microscopy (AFM, Nanoscope V by Digital Instruments). A commercial variable-temperature STM (Omicron Nanotechnology) was used for tunneling microscopy/spectroscopy. The thin film surface was thoroughly cleaned using isopropanol in an ultrasonic bath just before inserting it into the ultra-high vacuum (base pressure  $10^{-10}$  mbar) chamber. Topographic scans were obtained in the constant current mode ( $I = 0.3$  nA) by applying a bias voltage  $V$  in the range 0.7 – 0.8 V (positive for empty sample states). The differential tunneling conductance,  $G = dI/dV$ , was directly obtained using a lock-in amplifier and superimposing a modulation voltage of 0.1 V with a frequency of 1 kHz to the bias voltage. Measurements were carried out in the temperature range 40 – 300 K. STM/S was typically conducted over areas of  $50 \times 50 \text{ nm}^2$ , and spectroscopic scans were carried out with a lateral resolution of 1 nm (i.e., 2500 pixels). Reproducibility was confirmed by obtaining identical forward/backward and trace/retrace scans.

## 3. Results and discussion

The temperature dependence of the resistance  $R$  of the LCeMO thin films reveals a metal-insulator transition at  $T_{MI} \approx 260$  K, as seen in figure 1(a). In a field of 9 T, the magnetoresistance close to  $T_{MI}$  was found to be  $\sim 80\%$ . The temperature variation of

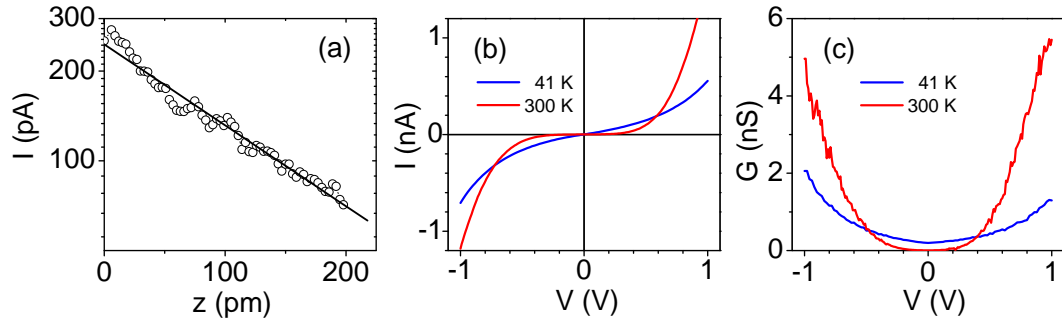


**Figure 2.** (a) Dependence of tunneling current  $I$  on relative tip-sample distance  $z$  on a semi-logarithmic scale. (b) Tunneling current vs bias voltage ( $I$ - $V$ ) curves averaged over an area of  $50 \times 50 \text{ nm}^2$  at 41 and 300 K displaying metallic and insulating behavior, respectively. (c) The corresponding conductance vs bias voltage ( $G$ - $V$ ) curves at 41 and 300 K.

magnetization in Figure 1(b) indicates a Curie temperature of  $T_C \sim 250 \text{ K}$ . A granular texture with average grain size of  $\sim 100 \text{ nm}$  can be inferred from the AFM images [cf. Figure 1(c)]. This suggests that epitaxial strain is relaxed at the film surface. In order to check the quality of our tunnel junctions, we measured repeatedly the  $I(z)$  characteristics on several spots. In Figure 2(a),  $I(z)$  is plotted on a semi-logarithmic plot. The exponential nature of  $I(z)$  confirms a good vacuum tunneling contact. The effective work function  $\phi$  was found to be  $\approx 1 \text{ eV}$  which clearly indicates that the tunnel junction is not contaminated [15]. The  $I$ - $V$  curves, Figure 2(b), measured at  $300 \text{ K} > T_{MI}$  exhibits an insulating gap at the Fermi energy  $E_F$ , i.e., close to the bias voltage  $V = 0$ . The corresponding  $G$ - $V$  curve denotes a zero-bias conductance  $G_0 = dI/dV|_{V=0} \simeq 0$  in Figure 2(c), implying the absence of states at  $E_F$  for the electrons to tunnel. In contrast, well below  $T_{MI}$ , at 41 K, the  $I$ - $V$  curve indicates metallic behavior. The  $G$ - $V$  curve at 41 K shows a finite  $G_0 \sim 0.2 \text{ nS}$ , i.e., occupied states at  $E_F$ .

In epitaxial thin films, substrate-induced strain and the granular structure are known to cause inhomogeneities in the local surface conductivity [16, 17]. These inhomogeneities can be directly mapped by spatially resolved STS. To see if the granular morphology of our films influences the local surface conductivity, we carried out topographic and spectroscopic scans of the same  $50 \times 50 \text{ nm}^2$  area simultaneously in the metallic state. One such result of a topographic scan at 41 K is presented in Figure 3(a). For comparison, the zero-bias conductance  $G_0$  of the same area is shown in Figure 3(b). Clearly, the elevated areas (e.g., the one marked 1) of the film appearing bright in the topography map correspond to regions with enhanced conductivity appearing green in the conductance map (also marked 1). On the other hand, depressed areas appearing dark in Figure 3(a) (marked 2) correspond to regions with low conductivity depicted blue (also marked 2) in Figure 3(b). The typical  $I$ - $V$  curves observed in the two regions are plotted in Figure 3(c). The slope at  $V \rightarrow 0$  of curve 1 is higher compared to that of curve 2 representing higher conductivity in region 1 than in region 2. Although curve 2 demonstrates less conducting behavior, it doesn't show an insulating gap. This is also evident from the zero-bias conductance histogram in Figure 3(d), which displays almost no weight at  $G_0 \sim 0$ . Moreover, this confirms that the inhomogeneity in the conductance map is likely not due to insulating oxide  $\text{CeO}_2$ . The associated length scale of this PS into high and low conducting regions is found to be several nanometers. This is in contrast to homogeneous conductance maps observed in the metallic state of  $\text{Pr}_{0.68}\text{Pb}_{0.32}\text{MnO}_3$  single crystals [18] but agrees with other investigations on strained films [6].

In conclusion, we confirmed by the STM/S that the granular film texture strongly influences

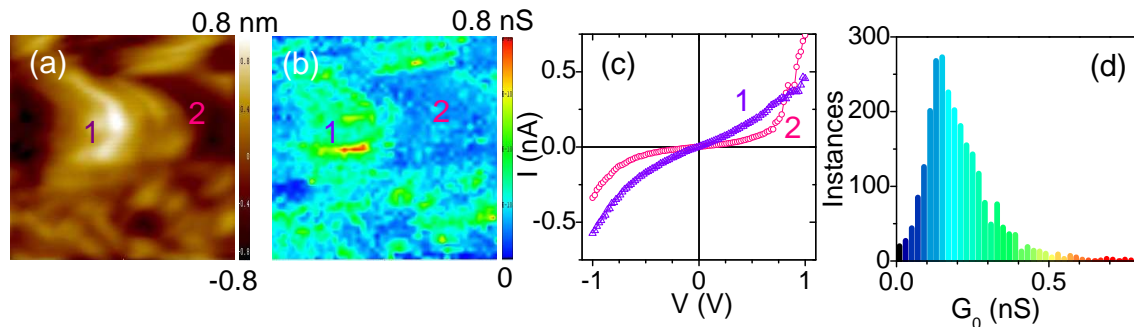


**Figure 3.** (a) STM topography of a LCeMO thin film over an area  $50 \times 50 \text{ nm}^2$  taken at 41 K. (b) The simultaneously obtained conductance map on the same area exhibits high conductance in region 1 and low conductance in region 2. (c) Typical  $I$ - $V$  curves seen in region 1 ( $\Delta$ ) and 2 ( $\circ$ ). (d) Histogram displaying the distribution of the zero-bias conductance  $G_0$ .

the local surface conductivities of electron doped  $\text{La}_{0.7}\text{Ce}_{0.3}\text{MnO}_3$ . The granularity and phase separation can also reflect some chemical inhomogeneity but no indication of insulating  $\text{CeO}_2$  is found. We suggest that the phase separation observed deep in the metallic state need not necessarily be an *intrinsic* material property of the manganites.

### Acknowledgments

We thank the DFG for financial support through grant WI 1324/1-1, and the European Commission through CoMePhS 517039.

### References

- [1] Raychaudhuri P, Mukherjee S, Nigam A K, John J, Vaisnav U D, Pinto R and Mandal P 1999 *J. Appl. Phys.* **86** 5718
- [2] Dagotto E 2002 *Nanoscale phase separation and colossal magnetoresistance* (Heidelberg:Springer)
- [3] Uehara M, Mori S, Chen C H and Cheong S -W 1999 *Nature (London)* **399** 560
- [4] Sarma D D, Topwal D, Manju U, Krishnakumar S R, Bertolo M, La Rosa S, Cautero G, Koo T Y, Sarma P A, Cheong S -W and Fujimori A 2004 *Phys. Rev. Lett.* **93** 097202
- [5] Fäth M, Freisem S, Menovsky A A, Tomioka Y, Aarts J and Mydosh J A 1999 *Science* **285** 1540
- [6] Becker T, Streng C, Luo Y, Moshnyaga V, Damaschke B, Shannon N and Samwer K 2002 *Phys. Rev. Lett.* **89** 23720
- [7] Mitra C, Raychaudhuri P, John J, Dhar S K, Nigam A K and Pinto R 2001 *J. Appl. Phys.* **89** 524
- [8] Yanagida T, Kanki T, Vilquin B, Tanaka H and Kawai T 2004 *Phys. Rev. B* **70** 184437
- [9] Stingl C, Moshnyaga V, Luo Y, Damaschke B, Samwer K and Seibt M 2007 *Appl. Phys. Lett.* **91** 132508
- [10] Chang W J, Hsieh C C, Juang J Y, Wu K H, Uen T M, Gou Y S, Hsu C H and Lin J -Y 2004 *J. Appl. Phys.* **96** 4357
- [11] Mitra C, Hu Z, Raychaudhuri P, Wirth S, Csiszar S I, Hsieh H H, Lin H J, Chen C T and Tjeng L H 2003 *Phys. Rev. B* **67** 092404
- [12] Han S W, Kang J S, Kim K H, Lee J D, Kim J H, Wi S C, Mitra C, Raychaudhuri P, Wirth S, Kim K J, Kim B S, Jeong J I, Kwon S K and Min B I 2004 *Phys. Rev. B* **69** 104406
- [13] Raychaudhuri P, Mitra C, Mann P D A and Wirth S 2003 *J. Appl. Phys.* **93** 8328
- [14] Chang W J, Tsai J Y, Jeng H T, Lin J Y, Zhang K Y J, Liu H L, Lee J M, Chen J M, Wu K H, Uen T M, Gou Y S and Juang J Y 2005 *Phys. Rev. B* **72** 132410
- [15] Renner Ch and Fischer Ø, 1995 *Phys. Rev. B* **51** 9208
- [16] Paranjape M, Raychaudhuri A K, Mathur N D and Blamire M G 2003 *Phys. Rev. B* **67** 214415
- [17] Sudheendra L, Moshnyaga V, Mishina E D, Damaschke B, Rasing T and Samwer K 2007 *Phys. Rev. B* **75** 172407
- [18] Rößler S, Ernst S, Padmanabhan B, Elizabeth S, Bhat H L, Wirth S and Steglich F 2007 *IEEE Trans. Magn.* **43** 3064